Research Signpost
Trivandrum
Kerala, India

Recent Advances in Pharmaceutical Sciences VIII, 2018: 59-78 ISBN: 978-81-308-0579-5
Editors: Diego Muñoz-Torrero, Yolanda Cajal and Joan Maria Llobet

# 4. Study of the transport of substances across the blood-brain barrier with the 8D3 anti-transferrin receptor antibody

Itsaso Cabezón[1], Elisabet Augé[1], Antoni Camins[2], Jordi Vilaplana[1] and Carme Pelegrí[1]

[1]*Secció de Fisiologia, Departament de Bioquímica i Fisiologia, Facultat de Farmàcia i Ciències de l'Alimentació, Universitat de Barcelona*
[2]*Departament de Farmacologia, Toxicologia i Química Terapèutica, Facultat de Farmàcia i Ciències de l'Alimentació, Universitat de Barcelona*

**Abstract.** Numerous strategies have been proposed to overcome the blood-brain barrier (BBB) and efficiently deliver therapeutic agents to the brain. One of these strategies consists of linking the pharmacologically active substance to a molecular vector that acts as a molecular *Trojan Horse* and is capable of crossing the BBB using a receptor-mediated transcellular transport system of the brain capillary endothelial cells (BCECs). The transferrin receptor (TfR) is related to a transcytosis process in these cells, and the 8D3 monoclonal antibody (mAb), directed against the mouse TfR, is able to induce a receptor response. Thus, the 8D3 antibody could be a potential molecular *Trojan Horse* to transport pharmacologically active substances across the BBB. On these bases, a series of experiments were performed where the 8D3 antibody was conjugated to different cargoes, the resulting constructs were administered *in vivo* to mice, and the

Correspondence/Reprint request: Dra. Carme Pelegrí, Secció de Fisiologia, Departament de Bioquímica i Fisiologia, Facultat de Farmàcia i Ciències de l'Alimentació, Universitat de Barcelona, Av. Joan XXIII 27-31, 08028 Barcelona. E-mail: carmepelegri@ub.edu

distribution and intracellular mechanisms that these constructs undergo at the BBB were studied. Our results indicated a TfR-mediated and clathrin-dependent internalization process by which the 8D3-cargo constructs enters the BCEC. The resulting endocytic vesicles follow at least two different routes. On one hand, most vesicles enter intracellular processes of vesicular fusion and rearrangement in which the cargo is guided to late endosomes, multivesicular bodies or lysosomes. On the other hand, a small but not negligible percentage of the vesicles follow a different route in which they fuse with the abluminal membrane and open towards the basal lamina, indicating a potential route for the delivery of therapeutic substances. In this route, however, the 8D3−cargo remain fixed to the abluminal membrane, indicating that the 8D3 is maintained linked to the TfR, and the cargo does not go beyond the basal membrane. Altogether, different optimization approaches need to be developed for efficient drug delivery, but receptor-mediated transport (RMT) continues to be one of the most promising strategies to overcome the BBB.

## Introduction

The blood-brain barrier (BBB) is a well-coordinated and highly selective barrier whose main function is to regulate brain homeostasis and the transport of endogenous and exogenous substances between the blood and the brain. It permits the selective brain uptake of nutrients and impedes the entrance of potentially harmful substances and pathogenic organisms into the brain [1-3]. Due to this restrictive nature of the BBB, the transport of therapeutics from the blood to the brain results extremely difficult, and has become a major pharmaceutical challenge in recent decades [1]. Only lipophilic molecules with a molecular mass under a 400-600 Da threshold are capable of crossing the BBB [1, 4]. Moreover, efflux transport systems such as P-glycoprotein, which are present in the brain capillary endothelial cells (BCECs), are able to export some of these small drugs back to the blood [5]. Hence, 98% of all small drugs and almost 100% of large molecule drugs are unable to cross the barrier [6].

Different strategies have been proposed to transport neurotherapeutics from the blood into the brain, including the utilization of the receptor-mediated transport (RMT) mechanisms present in the BCECs [1, 7]. The transferrin receptor (TfR), which is abundant in brain capillaries [7], has been extensively studied. Some monoclonal antibodies (mAbs) directed against this receptor have shown to be useful tools for studying TfR-mediated transcytosis across the BBB in rodents, and have been proposed as possible vectors or molecular *Trojan Horses* to transport substances across the BBB [8-14]. Some studies have concluded that anti-TfR mAbs accumulate in BCECS and do not cross the BBB, while other

studies, most of which have used the capillary depletion method or indirect outcome measures such as protein expression or enzymatic activity, have concluded that mAbs and/or their cargo are successfully transported across the BBB [8, 12, 14-16]. Thus, whether or not mAbs directed against the TfR undergo receptor-mediated transcytosis remains unclear (Figure 1).

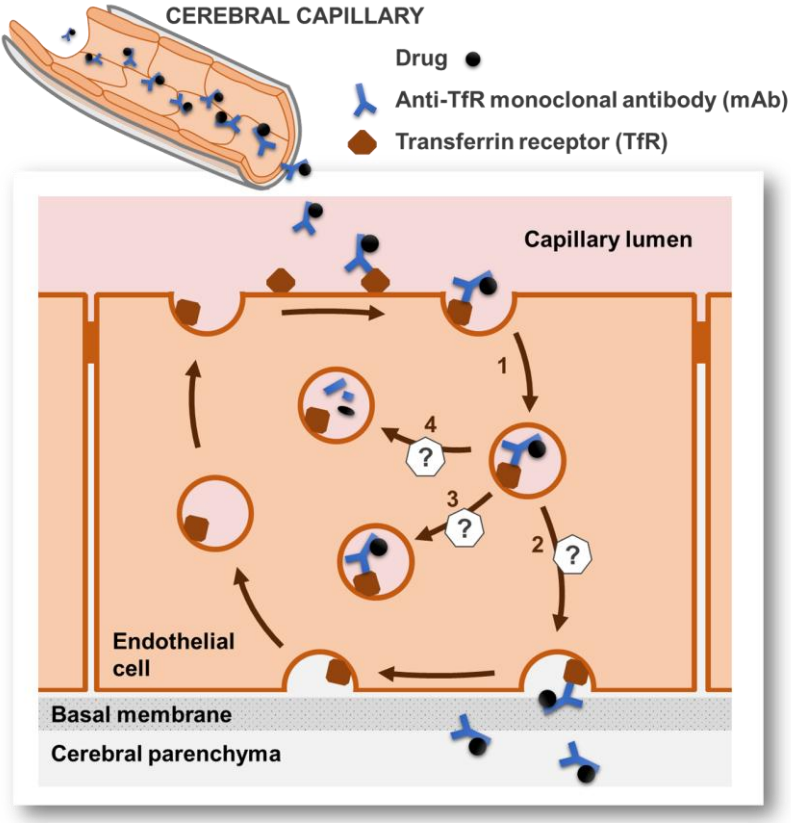


**Figure 1.** The proposed model for the transport of drugs across the BBB using RMT and anti-TfR mAbs includes: 1) the endocytosis of the drug-mAb/TfR on the luminal membrane and 2) the exocytosis of the mAb-drug on the basolateral membrane and receptor recycling. However, other possible destinations for the drug-mAb/TfR complex can be possible, as: 3) accumulation of the drug-mAb/receptor complex inside the BCEC, and 4) mAb and drug degradation.

The rat mAb 8D3, directed against the mouse TfR, has been proposed as a potential carrier candidate to transport substances across the mouse BBB. This mAb was first produced by Britta Engelhardt's research group in the Max Planck Institute (Bad Nauheim, Germany) [11], and some active substances that have been used as a cargo, seemed to achieve better results in crossing the BBB when attached to the 8D3 [14, 17-21]. However, the intracellular mechanisms the mAb or the mAb-cargo construct undergo inside BCECs still need to be elucidated.

The lack of more exhaustive analysis by means of microscopic techniques that allow the detection and direct localization of the mAb and / or cargo at a cellular and subcellular level, as well as the existing unknowledge regarding the cellular and intracellular processes that take part in the processing of these molecular *Trojan Horses* at the BBB level, have been the basis for the approach of this work.

In order to test the viability of the 8D3 as a potential carrier, a series of experiments were performed where the 8D3 antibody was conjugated to different cargoes, the resulting constructs were administered *in vivo* to mice, and the distribution and intracellular mechanisms that these constructs undergo at the BBB were studied.

## 1. The 8D3 antibody is able to recognize TfR and trigger the internalization of the cargo which is conjugated to [adapted from 22]

First of all, in order to test the reactivity of the 8D3 antibody for the TfR present in the luminal membrane of the BCECs, an inmmunohistochemical procedure was applied using 8D3 as the primary antibody on cryostat sections of mouse brain (male ICR-CD1). As expected, the staining permitted the visualization of brain capillaries (Figure 2A), where the BBB is present and the TfR is localized in the endothelial cells, but did not allow to visualize the vessels of the choroid plexus, in which the capillaries are fenestrated and the endothelial cells do not present TfR.

The second step was to test whether this antibody could be detected in brain capillaries after *in vivo* administration. For this purpose, a second group of animals underwent i.v. administration of 8D3 antibody in the caudal vein, and after 20 min of recirculation, brain samples were taken and localization of the 8D3 was determined via immunohistochemical techniques. The results showed that, in the same regions observed by direct immunohistochemistry, the brain capillaries contained the 8D3 antibody (Figure 2B1 and 2C1). They were stained with only the secondary antibody directed against 8D3, indicating that intravenously administered 8D3

antibody reaches and attaches to the BCECs. A simultaneous staining performed with laminin (a component of the basal membrane used to delimit the abluminal wall of the capillaries) showed that the laminin staining surrounded the 8D3 staining, suggesting that the antibody does not complete transcytosis, is unable to reach the cerebral parenchyma and remains inside the endothelial cell (Figure 2C3). It can also be observed that the 8D3 antibody presented a granular pattern (Figure 2C1 inset), which contrasted with the fine and smooth staining of the laminin (Figure 2C2 inset). This granular pattern suggested some endocytic process by which the antibody could have been internalized inside the BCEC.

After observing that the intravenously administered 8D3 antibody can be localized in the wall of the brain capillaries, our next goal was to develop an immunocomplex (IC) composed of the 8D3 antibody (molecular *Trojan Horse*) and Fab' fragments (that simulated a cargo) attached to the 8D3, and study the capacity of this antibody to transport the Fab' fragment across the BBB. A third group of animals received an i.v. injection of the 8D3-Fab' ICs in the optimal proportions established previously (1:4 weight/weight 8D3/Fab'). After different times of recirculation (2.5 h and 24 h, as 20 min seemed not enough to allow the mAb to cross the BBB),

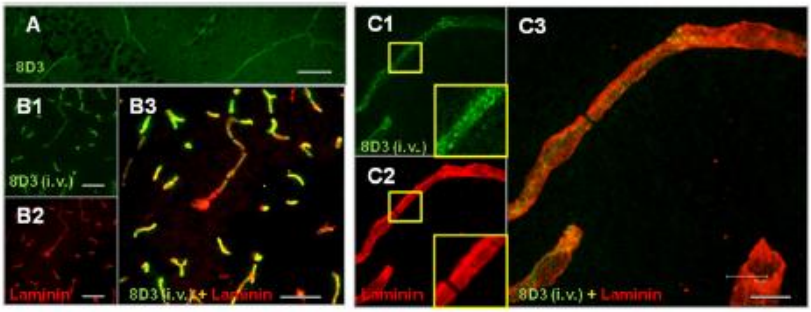


**Figure 2.** (A) Immunohistochemical labeling of mouse brain sections with the primary rat 8D3 MAb targeting murine TfR and the secondary AF488 anti-rat IgG (green color). (B and C) Brain sections from a representative mouse which received the 8D3 antibody intravenously. The sections were stained with an anti-laminin antibody as a primary, and both the AF555 (red color) and the AF488 anti-rat IgG (green color) as secondary antibodies to detect, respectively, the anti-laminin antibody and the administered 8D3. It can be observed that, after intravenous administration of 8D3, the antibody could be found in brain capillaries but not in parenchyma. The granular pattern of the 8D3 staining (C1 inset) contrasts with the uniform staining of the laminin (C2 inset). Scale bars: 10 µm. [adapted from 22].

brains were obtained in order to study the localization and colocalization of both components of the IC by immunohistochemistry. Using a fluorescence microscope, we observed that both components localized in the wall of the capillaries (Figure 3A1 and 3A2), with a clear granular pattern and high colocalization between the two stains (Figure 3A3), indicating that both components of the IC remain attached or at least where in the same endosomal compartment. The simultaneous staining with laminin (Figure 3B and C) demonstrated that both 8D3 and Fab' cargo get externally delimited by this marker. In control animals that received an i.v. injection of an IC formed by nonspecific rat IgG and Fab' fragments, also in a 1:4 ratio, neither

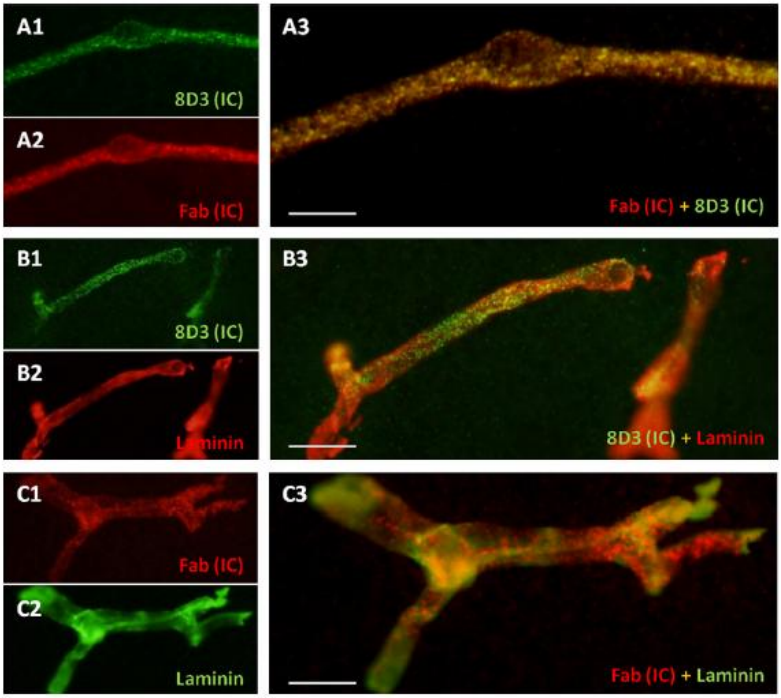


**Figure 3.** Localization of the components of the IC (8D3:Fab' 1:4) in brain capillaries of the hippocampus. (A) Localization of the 8D3 antibody with a secondary AF488 (green color) and of Fab' components with a secondary AF555 (red color). High colocalization (yellow color) of 8D3 and Fab' can be observed, and both components exhibit a granular pattern. (B and C) Simultaneous staining of laminin and 8D3 or Fab' components. 8D3 and Fab' seem to be localized inside the region delimited by the basal lamina. Scale bars: 10 µm. [adapted from 22].

the IgG nor the Fab' staining was observed in brain sections, hence indicating that the IC is not retained in the BCECs if it does not include an antibody directed against the TfR.

In order to study the maintenance and stability of the IC in the wall of the blood vessels through the different recirculation times tested (2.5 h vs 24 h), we used the Fluorescence Resonance Energy Transfer (FRET) technique. As the ICs are formed by 8D3 rat IgG and goat anti-rat IgG Fab' fragments, they can be simultaneously immunostained with AF488 donkey anti-rat IgG and AF555 donkey anti-goat IgG. Microscope images of AF488 emission (green color) directly stimulated by its excitation frequency (blue color), were taken before and after bleaching AF555. When AF555 is bleached, it is incapable of capturing the emission of the AF488 that is emitted near to it (energy transfer), and thus, the detection of the donor emission is increased with respect to the initial conditions (Figure 4).

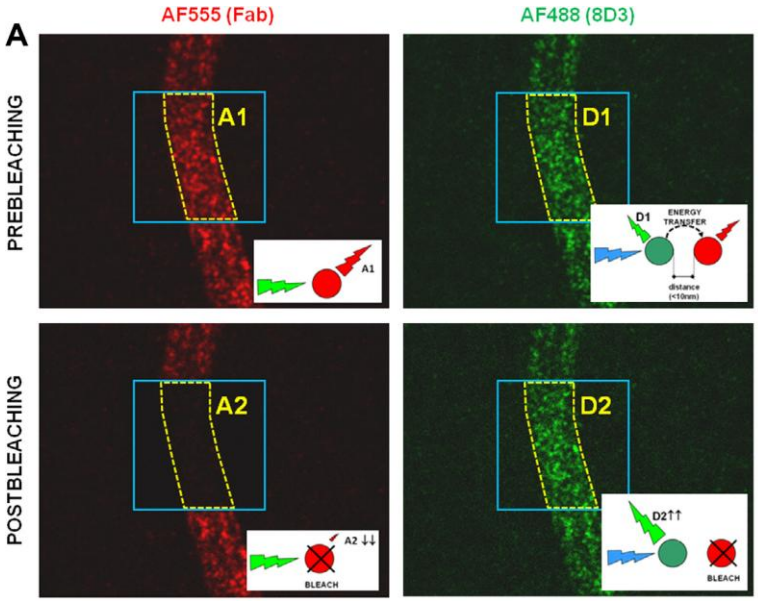


**Figure 4.** Process performed for one blood capillary using the FRET technique. When AF555 is bleached, it is incapable of capturing the green emission of the AF488 that is emitted near to it (energy transfer), and thus the observed donor emission (D2) after bleaching the AF555 is bigger than before bleaching (D1). A: acceptor emission, D: donor emission, 1: before bleaching, 2: after bleaching [adapted from 22].

Thus, by quantifying the increase of the detected donor emission, an indication of the number of molecules implicated in the energy transfer, i.e. molecules of AF488 and AF555 that are near one to the other, can be obtained. Statistical analysis indicated that the time of recirculation had a significant effect on the increase of the detected donor emission, being the increase higher in animals that were sacrificed 2.5 h after IC administration than in animals sacrificed 24 h later. As AF488 and AF555 stain respectively the 8D3 and the Fab' fragments, the increases also indicate the amount of 8D3 and Fab' fragments that persist attached on the original ICs. Thus, the colocalization of the fluorescent signals inside the endothelial cells decreased with time, indicating that ICs are processed and Fab' fragments probably separated from 8D3.

On the other hand, in order to directly visualize the 8D3 antibody and avoid the immunohistochemical processing, a fourth group of animals received an i.v. injection of 8D3 previously marked with fluorescein isothiocyanate ($8D3^{FITC}$). Likewise, another group of animals underwent i.v. administration of 8D3-Fab' ICs with FITC attached to Fab' ($8D3\text{-}Fab'^{FITC}$). Both $8D3^{FITC}$ (Figure 5) and $8D3\text{-}Fab'^{FITC}$ (data not shown) showed similar staining patterns in comparison with the anterior cases, being once again externally delimited by the laminin. However, a higher signal amplification was observed in the case of the $8D3\text{-}Fab'^{FITC}$ with respect to $8D3^{FITC}$, probably due to a bigger amount of FITC per 8D3 molecule.

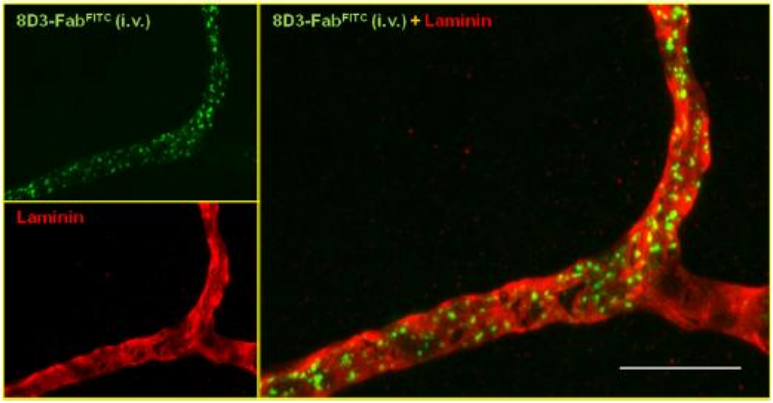


**Figure 5.** Localization of intravenously administered $8D3\text{-}Fab'^{FITC}$ (green color) and immunohistochemical staining with a primary antibody against laminin and secondary AF555 anti-rabbit IgG (red color) in brain capillaries of the hippocampus. The fluorescence of the administered IC is confined to the region delimited by laminin. Scale bar: 10 µm [adapted from 22].

As concluding remarks, we observed that the 8D3 antibody, with or without a cargo attached, is able to bind the TfR present in the luminal membrane of the BCECs and gets retained in these cells, probably in intracellular vesicles. Inside these cells, some kind of IC processing is produced, and after 24 h of recirculation, there were less Fab' fragments near the 8D3 molecules than after 2.5 h of recirculation. In any case, the components of the IC were never observed beyond the basal membrane or reaching the brain parenchyma. Thus, nor the 8D3 neither the IC seem to have completed transcytosis. These results cast doubt on the transcytotic capacity of the 8D3 antibody, and contradict previous studies that advocate an efficient transcytosis. However, the highest magnification level the optical microscopy allows us to work with, is perhaps not enough to draw a reliable conclusion, and we cannot rule out that an undetectable amount of antibody could have crossed the BBB.

## 2. 8D3-cargo constructs at the BBB: Intracellular mechanisms and subcellular localization [adapted from 23]

In view of the results obtained, the next step to move along in the study of the 8D3 antibody was to monitor in a more precise way the antibody localization and clarify which intracellular processes take part at the BBB.

For this purpose, gold nanoparticles (AuNPs) were coated with the 8D3 antibody, and using transmission electron microscope (TEM) techniques, the passage of these AuNPs across the BBB and their dynamics inside BCECs after *in vivo* administration were studied in mice. AuNPs not only can be directly observed by TEM, but also can be considered as the cargo to be transported by the 8D3. To form the 8D3-AuNP conjugates, the 8D3 antibody was covalently attached to AuNPs measuring 20 nm in diameter. The 8D3:AuNP ratio for the conjugates was approximately of 30:1. The conjugate was intravenously administered to ICR-CD1 mice that were distributed into four different groups, each of them with a different time of recirculation (10 min, 30 min, 2.5 h and 24 h). Once the corresponding time had passed, animals were anesthetized and intracardially perfused with paraformaldehyde and glutaraldehyde, and brains were then removed and processed for TEM.

Image analysis permitted the study of the AuNP localization at a subcellular level and at the different times of recirculation. The localization patterns varied over time. At the shortest time of recirculation (10 min), the AuNPs were mostly attached to the lumen of the capillary, in clathrin-coated pits or internalized in endocytic vesicles of the endothelial cells that

contained one or few AuNPs inside. The 8D3-AuNP conjugates are individually internalized, as no clathrin-coated pits containing more than one AuNPs were observed. No AuNPs were observed in the brains of the control mice, which had been administered with intravenous non-specific IgG-AuNP conjugate, confirming that the internalization depended on the presence of the 8D3. At 30 min of recirculation, the percentage of AuNPs yet to be internalized had decreased, and some of the intracellular vesicles contained a higher number of AuNPs. At the highest times of recirculation (2.5 h and 24 h), almost a 100% of the AuNPs observed had already been internalized in the BCECs, and many of the AuNP-containing vesicles had a higher number of particles inside them (up to 23 AuNPs in two cases). Some of the AuNPs were found in the basal lamina of the endothelium, bordering the abluminal membrane of the BCECs, which would suggest that 8D3-AuNP complex had completed transcytosis but remained attached to the TfR. Most of these AuNPs were observed at 2.5 h of recirculation, being 4.6% the percent respect to the total number of the AuNPs observed at this time (Figure 6).

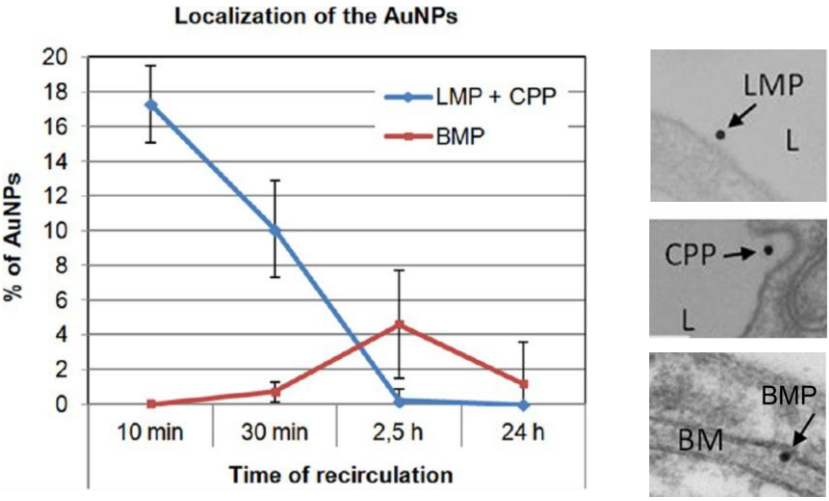


**Figure 6.** Percentage of AuNPs on the luminal surface [i.e. particles attached to the luminal membrane (LMP) and particles in clathrin-coated pits (CPP)] and basal membrane (BMP) for each recirculation time. Mean values and standard errors are shown. L: Lumen; BM: basal membrane. At 2.5 h of recirculation, all particles have been internalized, and the maximum percentage of particles that reach the basal membrane is obtained [adapted from 23].

Thus, at the shortest times of recirculation (10 min and 30 min), the predominant localization patterns were the lumen of the capillary, the clathrin-coated pits and the endocytic vesicles containing small amounts of AuNPs. Apart from the AuNPs that reach the basal lamina, the number of AuNPs per vesicle increased over time, so that at the longer times of recirculation, the vesicles containing high amounts of AuNPs was the main localization pattern (Figure 7).

The quantitative analysis performed with the data obtained permitted to establish and characterize a time-dependent trafficking pattern of endocytic internalization and endosomal processing of the conjugate at the BBB (Figure 8). The 8D3-AuNP conjugates are individually internalized within BCECs through a clathrin-dependent endocytosis process. The resulting AuNP-containing vesicles then follow at least two different routes. On one hand, most vesicles undergo intracellular processes of vesicular fusion and rearrangement in which the AuNPs end up accumulating in late endosomes, multivesicular bodies or lysosomes, which present a high AuNP content.

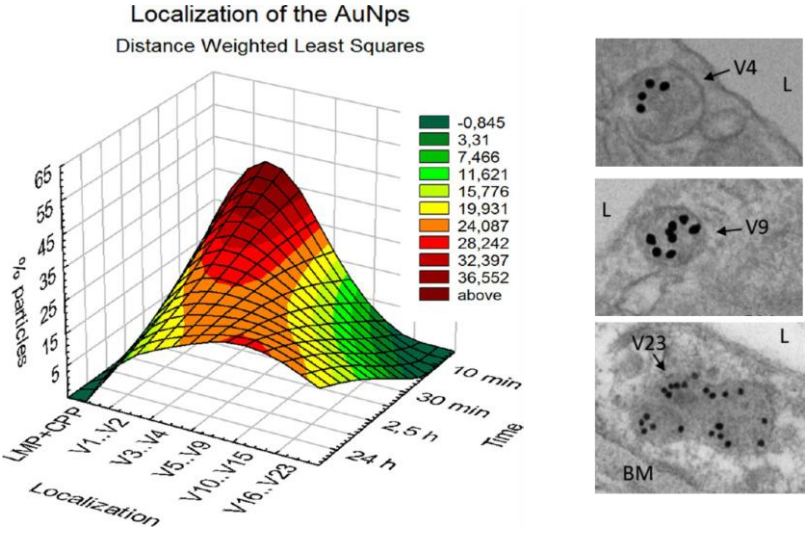


**Figure 7.** 3D contour graph obtained by adjusting, with distance weighted least-squares, the percentage of particles to the localization and the recirculation time. LMP: particles sited on luminal membrane; CPP: coated pit particles; V*i*: vesicle containing *i* AuNPs. Particles sited on basal membrane are not plotted. L: Lumen; BM: basal membrane [adapted from 23].

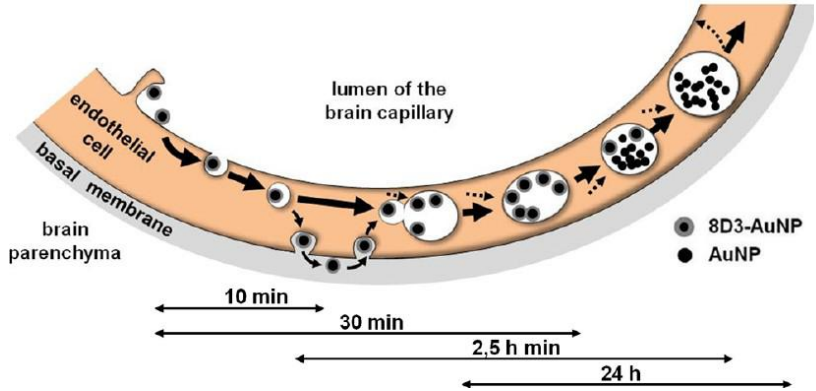


**Figure 8.** Deduced trafficking of the 8D3−AuNPs across the mouse BBB [adapted from 23].

On the other hand, a small percentage of vesicles (containing just one AuNP) follow a different route in which they fuse with the abluminal membrane and open to the basal lamina, which suggests an endosomal escape and transcytosis completion. However, the conjugates get retained in the basal lamina and do not reach the brain parenchyma.

Given the controversy regarding the possible use of anti-TfR antibodies to transport substances across the BBB, this study provided new information that may clarify some questions that are yet to be answered concerning the dynamics and intracellular processes the cargo undergo when coated with the 8D3 antibody. The results suggest that the 8D3 antibody may be a useful *Trojan Horse* to transport substances toward the BCECs. The 8D3 is able to drive the cargo to the brain capillaries and internalize it into the BCECs. This makes that a considerable amount of the intravenously administered cargo gets retained in the cerebral area instead of targeting another tissues or organs, and moreover, it makes the cargo to overcome the first barrier (the luminal membrane) reaching the inside of the endothelial cells. Although the cargo is mainly retained inside the BCEC, a small but not negligible percentage of particles escape from the conventional endosomal route, complete transcytosis and access the basal lamina, probably as a result of a different and uncommon endosomal sorting. This small percentage do not reach the brain parenchyma, perhaps due to the strong bond between the 8D3 and the TfR. Nevertheless, it should not be considered impossible for the cargo to reach the brain parenchyma once it has reached the basal lamina if

the linkage between the *Trojan Horse* and the transported cargo had properties that permitted the cargo to dissociate from the carrier.

## 3. Serial block-face scanning electron microscopy: A tool to three-dimensionally study the trafficking of mAb-cargo conjugates at the BBB [adapted from 25]

The results obtained by TEM provided relevant information at an ultrastructural level concerning the dynamics of the AuNPs when transported by the 8D3 antibody after *in vivo* administration. However, the two-dimensional (2D) image analysis entailed a series of limitations that we decided to overcome by carrying out a three-dimensional (3D) structural study that could give more insight into the transport of molecules across the BBB, and more knowledge on the trafficking of the AuNPs.

Serial block-face (SBF) imaging is a recently developed imaging technique that uses scanning electron microscopy (SEM) to acquire serial images and reconstruct large tissue regions in 3D [24]. In SBF-SEM, surface areas of the embedded tissue blocks are serially cut and removed with the built-in diamond knife in the SEM chamber between the cycles of SEM imaging. Because the consecutive areas of tissue are imaged with surface milling, this method generates largely pre-aligned images, which speeds up 3D reconstruction of the target structures. The objective of this work was first to determine whether the SBF-SEM resulted appropriate to reconstruct BBB segments and AuNP-containing endocytic vesicles, and if so, try to obtain additional information that would complement our previous 2D studies. This technique has been extensively used to explore the connectivity of the neural network, but only rarely to study the structure of the BBB, and no SBF-SEM data exist on the transport of molecules across this barrier.

To this end, we performed the same experimental design as for the 2D TEM study, but it was only reproduced at 2.5 h of recirculation (the time of recirculation where more diverse localization patterns were observed). After the mice brains were processed for SBF-SEM, the stained blocks were imaged using a Gatan 3View serial block-face imaging system installed on a FEI Quanta 250 FEG scanning electron microscope. The resulting datasets were assembled into volume files and aligned. 3D reconstruction of the desired structures was performed in image stacks using Imaris 8.0.2 and Imaris 7.2 software.

In a first attempt to perform a 3D reconstruction of the BBB and to observe the localization of the AuNPs, capillary segments (up to 10 μm long

along the z axis) from different brain samples were fully 3D rendered using low-magnification image stacks (10,000-25,000×). These image stacks were obtained using an incident electron beam with an energy of 2.3-2.4 kV and spot size 3, and a chamber pressure of 50 Pa was applied to scan across the samples at a pixel dwell time of 60 µs. This level of magnification allowed us to identify the cellular components that form the neurovascular unit, such as BCECs, the basal lamina, pericytes, astrocytes, and three-dimensionally reconstruct them by manually tracing the area in each plane and surface rendering next (Figure 9). However, the AuNPs could not be clearly visualized, neither inside nor outside endocytic vesicles. This was due, on one hand, to the low resolution in the *x*-*y* plane, and on the other hand, due to the backscattered electron signal. Moreover, it must be pointed that the presence of bare resin in the lumen of the capillary caused electrical charging of the sample, and consequently, tissue deterioration or breakage.

Due to these technical problems, a second attempt with higher magnification imaging (>30,000×) of the capillary segments was considered, avoiding the inclusion of the whole lumen in the region of interest (ROI). We used an incident electron beam with an energy of 3.5 kV and spot size 3, and a chamber pressure of 50 Pa was applied to scan across the samples at a pixel dwell time of 60 µs. At this level of magnification, BCEC segments and the basal lamina of the endothelium could be observed, as well as both the vesicles inside the BCECs and the AuNPs contained in them. The sequential images in the stack allowed us to 3D render structures such as the basal lamina or the vesicles located inside the BCECs by manually tracing the area in consecutive planes (Figure 10). Although the AuNPs were visible, due to their small size, it was impossible to 3D render them using this method; they are located in one or another section, but never in more than one, so it was impossible to reconstruct these particles in 3D by manually tracing the area across consecutive planes. Thus, a copy of the stack was preprocessed using the Fiji software to later replace the AuNPs in each section by 3D spheres of similar size (20 nm diameter) in Imaris. Since the AuNPs are the darkest structures in these images, they could be segmented with the Fiji software using a low threshold value. After segmentation, the resulting binary particles were split using a watershed to allow individual reconstruction. The final binary stack of images was loaded into Imaris as an additional channel of the original stack and the AuNPs were rendered as spheres in the final 3D reconstruction.

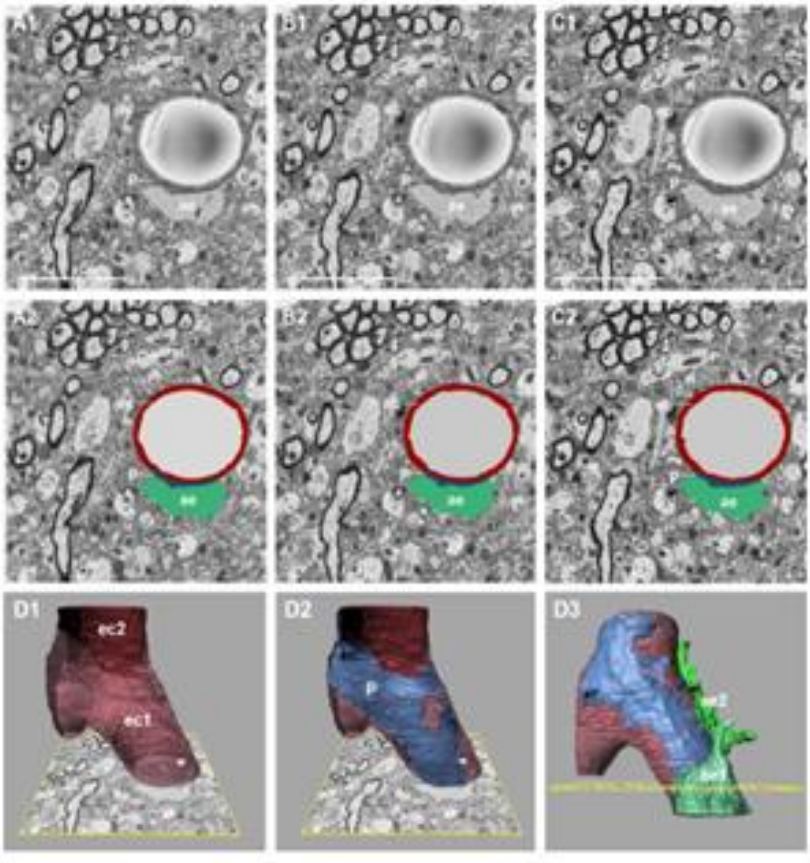


**Figure 9.** (A1-C1) Three selected serial images from an SBF-SEM low-magnification image stack. (A2-C2) Colored areas represent some of the structures that were selected and manually traced in A1-C1, respectively, for the subsequent 3D reconstruction. (D1-D3) Three snapshots of the video showing the 3D reconstruction: (D1) Two adjacent endothelial cells (ec1 and ec2) can be observed. Image B1 is superimposed on the reconstruction. (D2) A pericyte rendering is added to the reconstruction. (D3) The complete 3D reconstruction of the BBB segment, which includes the renderings of the two adjacent endothelial cells, the pericyte and two astrocytic endfeet (ae1 and ae2). Ec: endothelial cell; p: pericyte; ae: astrocytic endfeet. Scale bar: 5 µm [adapted from 25].

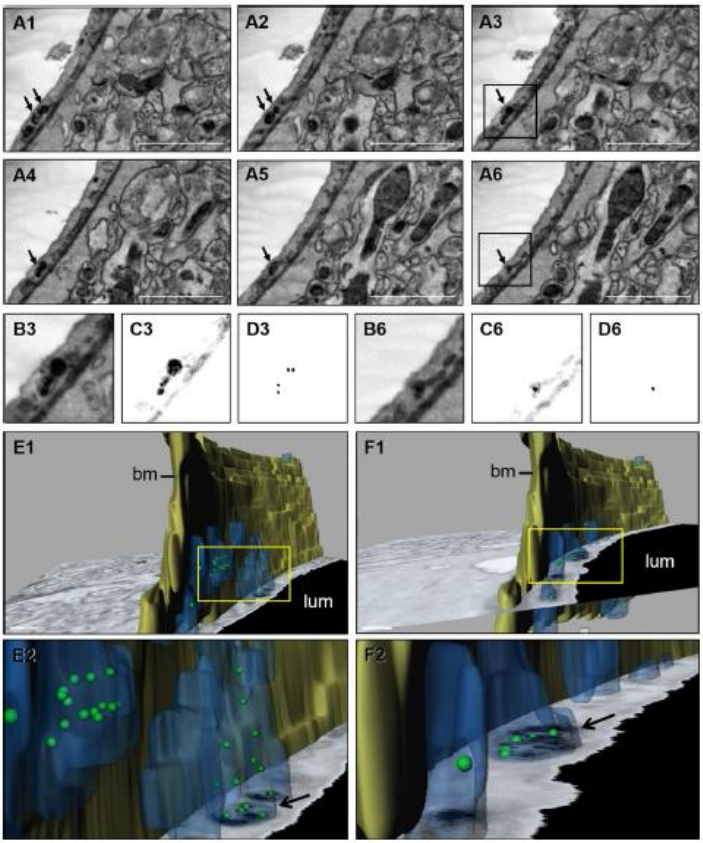


**Figure 10.** (A1-A6) Six selected serial images from an SBF-SEM high-magnification image stack. Arrows indicate the same vesicle sectioned on different planes. (B3-B6) Original insets from A3 and A6, respectively, in which the brightness and contrast have been modified to enhance visualization of the AuNPs. (D3 and D6) Images corresponding, respectively, to the insets from A3 and A6 that were obtained after applying the process of binarization, which permits to localize the AuNPs. (E1 and F1) Representative images of the 3D reconstruction of the SBF-SEM high-magnification image stack that contains images A1-A6. AuNPs are represented as green spheres. Blue regions are the endothelial vesicles. bm: basal lamina; lum: lumen of the capillary. (E2 and F2) Insets from E1 and F1, respectively. Arrow in E2 indicates some AuNPs that have lost the connection with the vesicular membrane, while in F2 it shows some ones in which the connection is maintained. Scale bar: 2 µm [adapted from 25].

Thus, this level of magnification and this strategy allowed for reliable 3D reconstructions in which the structures of the BBB, such as the basal lamina of the endothelium and the vesicles located in the BCECs, as well as the precise location of the AuNPs could be visualized simultaneously (Figure 10).

Regarding the shape of the vesicles, the 3D reconstruction allowed us to observe that although some of the AuNP-containing vesicles present a spherical or ellipsoidal form, they are often branched structures with irregular shapes, which sometimes even seem to merge with each other forming a complex endosomal network. As can be observed in Figure 10, some vesicles that show a spherical or ellipsoidal shape in a 2D plane can be considered part of a complex and irregular when subsequent sections are analyzed as a whole 3D structure.

We can conclude from this work that low-magnification imaging permits acquiring images of a large field of view and monitoring of relatively long capillary segments (more than 10 µm long), so that results appropriate for the identification and 3D reconstruction of cellular elements and some subcellular elements as nuclei. However, this resolution was too low for clear identification of the AuNPs. This led us to increase the level of magnification and re-establish the setting parameters for the SBF-SEM system. A higher accelerating voltage allowed the acquisition of higher magnification images, with sufficient resolution for AuNP visualization. We therefore achieved the goal of 3D reconstructing BBB segments and AuNP-containing vesicles, as well as precisely localizing the AuNPs within the cellular structures. We observed that the vesicles containing AuNPs are often branched structures with irregular shapes, which sometimes even seem to merge with each other forming a complex endosomal network. Moreover, we applied an innovative method by which the AuNPs were replaced by 3D spheres of similar size at the exact same coordinates inside the tissue volume.

## 4. Conclusion

Altogether, the different studies exposed in the present work, allowed us to clarify some doubtful aspects concerning the transport of drugs across the BBB using RMT and anti-TfR mAbs. These aspects, which are summarized in Figure 11, permit to conclude that:

1. The 8D3 antibody is capable of recognizing and binding to the TfR present in the luminal membrane of brain capillary endothelial cells following *in vivo* administration.
2. The 8D3 antibody is internalized inside the brain capillary endothelial cells after its binding to the TfR.
3. The 8D3 antibody is able to trigger the internalization of the cargo which is conjugated to, overcoming the first obstacle in the transport across the brain capillary endothelial cells.
4. The internalized cargo can vary in size and nature, ranging from proteins like the Fab' fragments of antibodies to larger particles like AuNPs measuring 20 nm in diameter.
5. The internalization of 8D3 and its cargo is produced by a clathrin-dependent endocytosis process.
6. Most of the resulting endocytic vesicles undergo a process of fusion, maturation and reorganization in which the 8D3-cargo complexes that are inside them progressively accumulate in endosomal networks of great complexity.
7. During the processing of these vesicles the interaction between TfR, 8D3 and/or cargo is lost.
8. Nonetheless, some endocytic vesicles containing the 8D3-cargo complexes complete transcytosis.
9. These vesicles fuse with the basolateral membrane and open up to the basal lamina.
10. When fused with the basolateral membrane, the 8D3-cargo complexes become exposed to the basal lamina.
11. Exposed 8D3-cargo complexes remain attached to the TfR and fail to go beyond the basal lamina.
12. In order to facilitate the cargo liberation to the brain parenchyma, it is necessary to modify and optimize the linkages between the 8D3 and the cargo and/or the linkage between the 8D3 and the TfR.
13. Although some improvements at the design level of the constructs are needed, the use of the RMT system and mAbs directed against transcytosis receptors is a strategy with great potential for transporting drugs through the BBB.

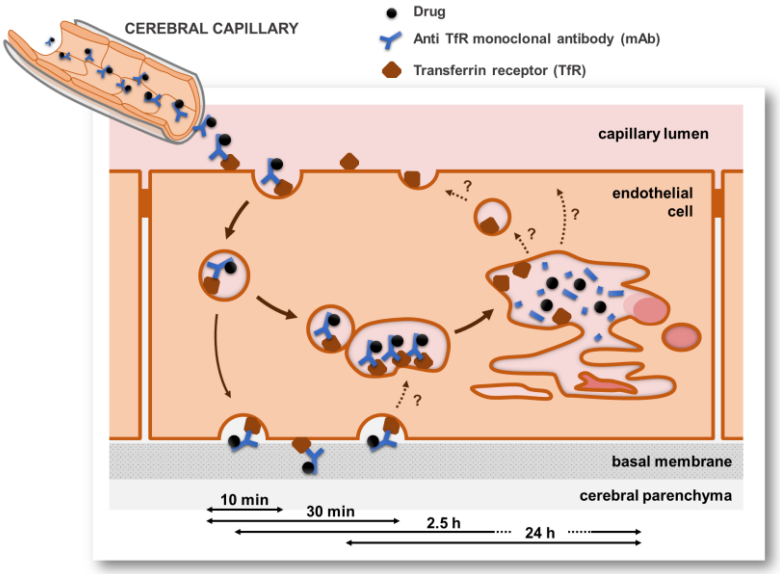


**Figure 11.** State of the art of both the transport of drugs across the BBB using anti-TfR mAbs and the possible destinations for the drug-mAb/TfR complexes.

## Acknowledgements

This work is a summary of the doctorate thesis of Itsaso Cabezón, carried out in the Blood Brain Barrier Research Group from the Universitat de Barcelona (http://hdl.handle.net/2445/110075).

## References

1. de Boer, A. G., Gaillard, P. J. 2007, *Annu. Rev. Pharmacol. Toxicol.*, 47, 323.
2. Correale, J., Villa, A. 2009, *Neurochem. Res.*, 34, 2067.
3. Chen, Y., Liu, L. 2012, *Adv. Drug Deliv. Rev.*, 64, 640.
4. Pardridge, W. M. 1998, *J. Neurochem.*, 70, 1781.
5. Begley, D. J. 1996, *J. Pharm. Pharmacol.*, 48, 136.
6. Pardridge, W. M. 2005, *NeuroRX*, 2, 3.
7. Scherrmann, J. M. 2002, *Vasc. Pharmacol.*, 38, 349.
8. Jefferies, W. A., Brandon, M. R., Hunt, S. V., Williams, A. F., Gatter, K. C., Mason, D. 1984, *Nature*, 312, 162.
9. Friden, P. M., Walus, L. R., Musso, G. F., Taylor, M. A., Malfroy, B., Starzyk, R. M. 1991, *Proc. Natl. Acad. Sci. U. S. A.*, 88, 4771.

10. Moss, T. 1996, *J. Comp. Neurol.*, 375, 675.
11. Kissel, K., Hamm, S., Schulz, M. 1998, *Histochem. Cell Biol.*, 110, 63.
12. Lee, H. J., Engelhardt, B., Lesley, J., Bickel, U., Pardridge, W. M. 2000, *J. Pharmacol. Exp. Ther.*, 292, 1048.
13. Moos, T., Morgan, E. H. 2001, *J. Neurochem.*, 79, 119.
14. Zhang, Y., Pardridge, W. M. 2005, *J. Pharmacol. Exp. Ther.*, 313, 1075.
15. Shi, N., Pardridge, W. M. 2000, *Proc. Natl. Acad. Sci. U. S. A.*, 97, 7567.
16. Alata, W., Paris-Robidas, S., Emond, V., Bourasset, F., Calon, F. 2014, *Mol. Pharmaceutics*, 11, 243.
17. Shi, N., Zhang, Y., Zhu, C., Boado, R. J., Pardridge, W. M. 2001, *Proc. Natl. Acad. Sci. U. S. A.*, 98, 12754.
18. Lee, H. J., Zhang, Y., Zhu, C., Duff, K., Pardridge, W. M. 2002, *J. Cereb. Blood Flow Metab.*, 22, 223.
19. Zhu, C., Zhang, Y., Zhang, Y. F., Li, J. Y., Boado, R. J., Pardridge, W. M. 2004, *J. Gene Med.*, 6, 906.
20. Rivest, V., Phivilay, A., Julien, C., Bélanger, S., Tremblay, C., Émond, V., Calon, F. 2007, *Pharm. Res.*, 24, 981.
21. Boado, R. J., Zhang, Y., Wang, Y., Pardridge, W. M. 2009, *Biotechnol. Bioeng.*, 102, 1251.
22. Manich, G., Cabezón, I., Del Valle, J., Duran-Vilaregut, J., Camins, A., Pallàs, M., Pelegrí, C., Vilaplana, J. 2013, *Eur. J. Pharm. Sci.*, 49, 556.
23. Cabezón, I., Manich, G., Martín-Venegas, R., Camins, A., Pelegrí, C., Vilaplana, J. 2015, *Mol. Pharmaceutics*, 12, 4137.
24. Ohno, N., Katoh, M., Saitoh, Y., Saitoh, S., Ohno, S. 2015, *Microscopy*, 64, 17.
25. Cabezón, I., Augé, E., Bosch, M., Beckett, A. J., Prior, I. A., Pelegrí, C., Vilaplana, J. 2017, *Histochem. Cell Biol.*, 148, 3.